Modulation of the Expression of an Apical Plasma Membrane Protein of Madin-Darby Canine Kidney Epithelial Cells: Cell-Cell Interactions Control the Appearance of a Novel Intracellular Storage Compartment

Dora E. Vega-Salas, Pedro J. I. Salas, and Enrique Rodriguez-Boulan

Department of Cell Biology and Anatomy, Cornell University Medical College, New York, New York 10021

Abstract. Experimental conditions that abolish or reduce to a minimum intercellular contacts between Madin-Darby canine kidney epithelial cells result in the appearance of an intracellular storage compartment for apical membrane proteins. Subconfluent culture, incubation in 1-5 μM Ca^{++}, or inclusion of dissociated cells within agarose or collagen gels all caused the intracellular accumulation of a 184-kD apical membrane protein within large (0.5-5 μm) vacuoles, rich in microvilli. Influenza virus hemagglutinin, an apically targeted viral glycoprotein, is concentrated within these structures but the basolateral glycoprotein G of vesicular stomatitis virus and a cellular basolateral 63-kD membrane protein of Madin-Darby canine kidney cells were excluded. This novel epithelial organelle (VAC), which we designate the vacuolar apical compartment, may play an as yet unrecognized role in the biogenesis of the apical plasma membrane during the differentiation of normal epithelia.

During growth and differentiation, epithelial cells establish contact with other cells and with various extracellular matrix (ECM)[1] components which, in many instances, they synthesize themselves. There is considerable evidence that cell-substratum interactions promote or stabilize the expression of genes carrying out differentiated cellular functions. For example, ECM components promote growth and differentiation of mammary epithelial cells (17, 67), promote casein gene expression and secretion (32, 33), and regulate the nature and distribution of glycosaminoglycans (47). Likewise, ECM regulates hepatocyte proliferation and differentiation (18, 21). Hay and co-workers have shown that collagen and other ECM components stimulate differentiation and ECM synthesis by corneal epithelium (27, 37-39, 59). In fibroblasts, both messenger translatability and the synthesis of cytoskeletal components require cell-substratum interactions (4, 19).

The role of cell-cell contacts in the process of cell differentiation is not well defined. There is evidence that cell-cell interactions control cytoskeletal protein synthesis in epithelial cells (3), mammary epithelial cell differentiation (34), and endothelial cell growth (28). In *Dictyostelium*, synthesis and stability of mRNA are regulated by cell-cell contact (12). In epithelial cells in culture, the levels of expression of apical markers of differentiation, such as Na^+-dependent hexose transport and various hydrolase activities, increase markedly when the cells become confluent (1, 43, 49, 68). Even cilia and microvilli, typical morphological markers of the apical surface, are infrequent in subconfluent cells but are readily expressed on the apical surface as soon as the cells become confluent (42, 43).

This study explores regulatory aspects of the biogenesis of the apical membrane components in polarized Madin-Darby canine kidney (MDCK) epithelial cells, derived from dog kidney (9, 51, 58). It reports a novel mechanism used by epithelial cells to regulate the surface expression of apical markers: intracellular storage. We show that under conditions that abolish cell-cell contacts (subconfluence, low Ca^{++} levels) large amounts of apical plasma membrane proteins synthesized by the cell are prevented from reaching the cell surface and stored in a previously undescribed intracellular organelle with characteristics of apical plasmalemma. Culture procedures that dissociate cell-cell from cell-substratum interactions (23, 64) demonstrate that both types of contacts act independently in determining the final surface levels of apical protein.

Materials and Methods

Cell Culture

All experiments were carried out on MDCK cells (strain II) between passages 58 and 75. The cells were grown in 75-cm^2 tissue culture flasks (Fal-

1. *Abbreviations used in this paper*: ECM, extracellular matrix; RIA, radioimmunoassay; VAC, vacuolar apical compartment.

con Labware, Oxnard, CA) using Dulbecco's modified Eagle's medium (DME) (Gibco, Grand Island, NY), supplemented with 10% (vol/vol) horse serum (HyClone Laboratories, Logan, UT) in a humidified environment of 95% air, 5% CO_2 at 37°C. Cells were dissociated and replated once a week by treatment with 0.25% trypsin/0.2 mM EDTA. Under experimental conditions, the cells were incubated in the following serum-free media: DME (1.8 mM Ca^{++}, 1 mM phosphate); spinner medium (S-MEM) (1–5 μM Ca^{++}, 10 mM phosphate). In some experiments, the cells were included in 3% ultralow gelling point agarose (Seaprep, FMC, Rockland, ME), or native rat collagen gel, prepared as described by Elsdale and Bard (16), in any of the media described above. For incubation within gel/medium environments, the cells were dissociated with trypsin/EDTA and resuspended in serum-free 2× DME or 2× S-MEM, and immediately mixed with an equal volume of 6% ultralow gelling point agarose in water, or 4 mg/ml native collagen in 20 mM acetic acid neutralized with 0.34 M NaOH. Aliquots of this suspension containing ~9 × 10^4 cells were plated on top of thick agarose layers formed in 50-well detachable petri dishes (Lux, Miles), allowed to gel at 4°C for 10 min, and incubated for 24 h at 37°C.

Experiments with confluent monolayers were carried out with cells plated at saturation density (>250,000 cells/cm^2) on native collagen gels prepared as described above.

Experiments involving infection with influenza and vesicular stomatitis virus (VSV) temperature-sensitive mutants (ts61 and ts045, respectively) were performed as described elsewhere (52, 54).

Hybridoma Procedures

Female BALB/c mice (6–12 wk old) (Charles River Breeding Laboratories, Inc., Wilmington, MA) were inoculated intraperitoneally with ~2 × 10^6 MDCK cells that had been grown on culture beads (cytospheres; Miles Laboratories Inc., Elkhart, IN) and fixed with 2% paraformaldehyde. 0.5–1.0 × 10^8 NS-1 mouse myeloma cells were fused with preimmunized donor spleen lymphocytes using polyethylene glycol (4,000 mol wt, Merck). The fused cells were plated on spleen feeder layers in ten 96-well tissue culture clusters (Costar, Cambridge, MA) in RPMI 1640 medium (Gibco) supplemented with 10% FCS (Gibco) and 2% HAT (hypoxantine/aminopterin/thymidine (Sigma Chemical Co., St. Louis, MO). The cells were kept for 2–3 wk, subcloned by dilution, and the supernatants were screened for anti-MDCK cell surface activity by ELISA, immunofluorescence, and radioimmunoassay (RIA).

The cellular antigens for the mAbs were identified by immunoblot of postnuclear supernatants of MDCK cells (extracted with 0.1% Na deoxycholate, 0.5% Nonidet P-40, 1 mM phenylmethylsulfonyl fluoride [PMSF], 1 mM aprotinin, and 1 mM pepstatin) run in SDS PAGE, as described by Towbin et al. (61).

Immunofluorescence and RIA

Procedures for immunofluorescence and RIA have been described elsewhere (54, 55). Briefly, the cells were grown on thin collagen layers on glass coverslips (for immunofluorescence) or detachable 50-well plastic petri dishes (for RIA) (Lux; Miles Laboratories Inc.), fixed in 2% paraformaldehyde for 1 h and washed in PBS. The free aldehyde groups were quenched with 50 mM NH_4Cl in PBS and the cells were preincubated with 1% BSA and 50 μg/ml of preimmune IgG from the same species as the second antibodies (usually goat) in PBS. In the first step, the cells were incubated with mAb for 20 min and washed with 1% BSA in PBS. In the second step, rhodamine- or fluorescein-labeled, affinity-purified goat anti-mouse IgG (CooperBiomedical, Inc., Malvern, PA) were used for 20 min. The processing of cells included in gels was similar except that each step took 2 h. After five washes in PBS, the cells were mounted on a drop of 20% polyvinyl alcohol (Gelvatol, Monsanto, Indian Orchard Mass), 15% glycerol in PBS. When fluorescein was used, 5% *n*-propyl gallate was added to reduce photobleaching (22). Samples were photographed with a Leitz Ortholux epifluorescence microscope using Kodak Tri-X 400 ASA film. The range of exposure times was 30 to 80 s. For RIA, a [^{125}I]goat anti-mouse IgG was used as second antibody and each well counted separately in a gamma counter (Hewlett-Packard Co., Palo Alto, CA).

Semi-thin Frozen Sections

Confluent MDCK monolayers cultured on native collagen gels for 36 h were fixed in 2% paraformaldehyde/0.1% glutaraldehyde in PBS, scraped with a razor blade, and embedded in 10% gelatin–PBS. After infusion with 1.8 M sucrose for 12 h at 4°C the gels were frozen in liquid N_2 and sectioned with an ultracryomicrotome (model MT5000; Sorvall Instruments) at −85°C. The 0.5-μm sections were collected on glass coverslips pretreated with 1 mg/ml poly-L-lysine (Sigma Chemical Co.) and processed for indirect immunofluorescence as described above.

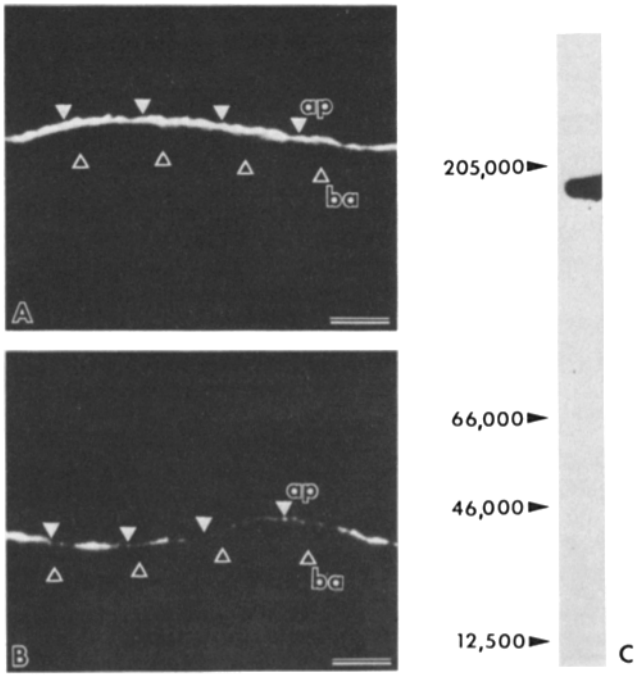

Figure 1. Apical localization of the 184-kD protein in confluent MDCK monolayers. Confluent monolayers of MDCK cells were cultured for 36 h on native collagen gels in (*A*) DME (1.8 mM Ca^{++}), or (*B*) S-MEM (1–5 μM Ca^{++}) and fixed in 2% paraformaldehyde, 0.1% glutaraldehyde in PBS. Semi-thin frozen sections (0.5 μm) were processed for indirect immunofluorescence with S2/2Gl monoclonal antibody and affinity-purified rhodaminated goat anti-mouse IgG. (*C*) Immunoblot of MDCK postnuclear supernatant processed with S2/2Gl monoclonal antibody, affinity-purified rabbit anti-mouse IgG and ^{125}I-labeled Protein A. The autoradiogram showed a single band of M_r 184,000. Note that monolayers confluent in both normal or low Ca^{++} concentration show polarization of the 184-kD membrane protein to the apical plasma membrane domain. Bars, 10 μm.

Immunoelectronmicroscopy

The immunoperoxidase procedure was a slight modification of the one described in detail by Brown and Farquhar (7). MDCK cell monolayers on native collagen gels were incubated in the presence of 1 mg/ml cationized ferritin (Sigma Chemical Co.) in normal medium for 30 min at 14°C before fixation. The cells were fixed in 2% paraformaldehyde/0.1% glutaraldehyde in PBS, and made permeable to antibodies with 0.1% saponin; 0.05% saponin was present in all subsequent incubations. The second antibody was affinity-purified goat (Fab fragment) anti-rabbit IgG, coupled to horseradish peroxidase (Biosys, Paris, France). Processing for electron microscopy included osmium postfixation, alcohol dehydration, and Epon embedding. Sections were observed and photographed with a JEOL 100 CX electron microscope.

The methods for morphometric measurements have been extensively described by others (66) and in a previous work (64). The estimation of the number of vacuoles per cell was obtained from the number of structures/volume density (N_v) as described by Weibel (66) as $N_v = N_a/D$, where N_a is the number/area density and D is the average caliper diameter. D was estimated as described by Hilliard (30) for prolate spheroids.

Intracellular Calcium Determinations

The procedure for intracellular calcium determination has been described by Tsien et al. (63). Briefly, MDCK cells were dissociated and kept in sus-

pension culture in serum-free DME (with no phenol red), 0.2% BSA for 14 h as described elsewhere (55). Before starting the experiment, the number of cells in the suspension was measured and only suspensions with >90% trypan blue-excluding cells were used. Approximately 10^5 cells in 0.5-ml samples were incubated with 50 μM quin2 acetoxymethyl ester (Calbiochem-Behring Corp., La Jolla, CA) from a 50-mM stock solution in DMSO) for 30 min at 37°C. The cells were spun and resuspended in protein-free, phenol red-free DME or S-MEM. The fluorescence from cell suspensions was measured with a fluorimeter set at 340 and 500 nm for excitation and emission, respectively. Maximal quin2 fluorescence was determined by addition of 0.1% Triton X-100 and minimal fluorescence by subsequent addition of 2 mM EGTA.

Results

The Intracellular Pool of the 184-kD Apical Surface Protein of MDCK Cells Is Very Small in Normal Confluent Monolayers

A mAb raised against the surface of MDCK cells, S2/2G1 (65), recognizes an apical protein of M_r 184,000 (Fig. 1 *A*), which is sensitive to treatment with trypsin/EDTA. Indirect RIA using S2/2G1 as first mAb and ^{125}I goat-labeled anti-mouse as second antibody demonstrated that only 10% of the binding activity of control confluent monolayers remains in cells plated immediately after trypsinization (Fig. 2 *A*, time 0). 100% binding was restored within the initial 24 h of incubation in DME (solid circles in Fig. 2 *A*). The total (surface + intracellular) pool of the 184-kD protein, determined in parallel monolayers treated with detergent after fixation (0.2% Triton X-100), was only slightly larger than the amount on the apical surface (x in Fig. 2 *A*). Thus, the intracellular pool (total − surface) of this apical antigen is very small in normal confluent monolayers of MDCK cells.

A Large Proportion of the 184-kD Protein Is Intracellular in MDCK Monolayers with Abolished Cell–Cell Interactions

Previous work (23, 64) has shown that MDCK monolayers kept in medium containing 1–5 μM Ca^{++} (1/1,000th the level of normal medium) do not develop normal cell–cell interactions. Tight junctions and the lateral domain are abolished and the cells have a striking dome-shaped appearance. In these "open" monolayers, the 184-kD protein is still expressed on the apical surface, although at reduced levels (Fig. 1 *B*). Quantitation by RIA demonstrated that, as in control monolayers, the surface expression of the 184-kD protein also reached a plateau within the initial 24 h of incubation after trypsin/EDTA treatment and plating (solid squares in Fig. 2 *B*). Plateau values were only ~40% of the level of surface expression found in control monolayers (solid circles in Fig. 2 *B*). Almost all of the remaining 60% was intracellularly stored antigen, as shown by RIA in the presence of detergent (open squares in Fig. 2 *B*). These results indicate that the 184-kD protein is produced by open monolayers at about the same rate as control monolayers but over half of the antigen is prevented from reaching the cell surface in the first case.

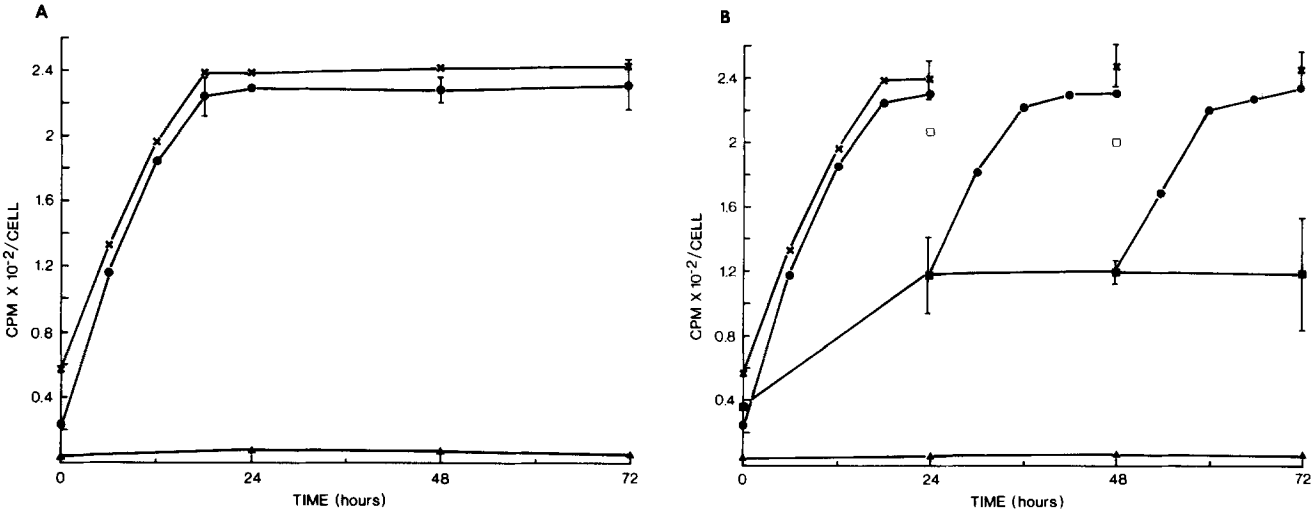

Figure 2. Quantitation of surface and intracellular 184-kD protein by indirect RIA in MDCK monolayers incubated in DME: effect of 1–5 μM Ca^{++}. (*A*) MDCK cells dissociated with trypsin/EDTA were immediately plated on native collagen gels in detachable wells in DME and fixed in 2% paraformaldehyde/0.1% glutaraldehyde at various times after plating (time 0 was 90 min after plating). The amounts of apical surface (●) and total cellular (x) 184-kD protein (the latter measured in monolayers treated with 0.2% Triton X-100) were determined by indirect RIA using mAb S2/2G1 and affinity-purified [^{125}I]goat anti-mouse IgG. Parallel control monolayers were processed with myeloma supernatant and iodinated second antibody (▲). Each point is the average of four independent experiments (quintuplicate monolayers). (*B*) MDCK cells were dissociated with trypsin/EDTA and immediately plated on native collagen gels in DME. At time 0 (90 min after plating) some monolayers were transferred to S-MEM (1–5 μM Ca^{++}) (■,□) while others were kept in DME (1.8 mM Ca^{++}) (●,x). After 24 or 48 h, a number of the monolayers kept in S-MEM were transferred to DME (●,x). The monolayers were fixed at various times in 2% paraformaldehyde, 0.1% glutaraldehyde in PBS—some were treated with Triton X-100 (x,□)—and processed for indirect RIA with S2/2G1 monoclonal antibody or myeloma supernatant (▲), as described in *A*. Note that the surface amount of 184-kD protein in cells kept in low calcium medium was ~40% of the amount expressed in cells kept in normal calcium medium. Note also that the intracellular pool of 184-kD protein (the difference between the amounts found in detergent-treated and untreated cells) was much larger in cells kept in low calcium medium.

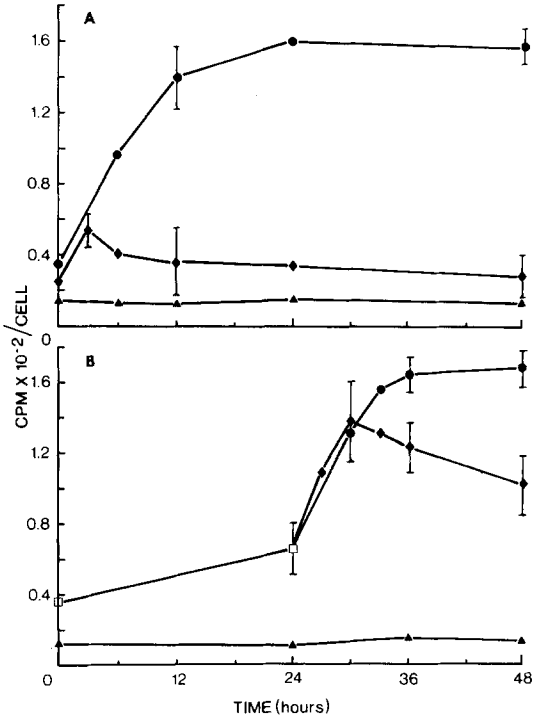

Figure 3. Effect of cycloheximide on the surface expression of the 184-kD protein. MDCK cells were dissociated and plated as described in the legend to Fig. 2. The surface expression of the 184-kD membrane protein was determined by indirect RIA as described in the legend to Fig. 2. Negative controls were carried out using myeloma supernatant as first antibody (▲). Each point is the average of three independent experiments (quintuplicate monolayers for each). Cycloheximide (17 μM) added at time 0 (90 min after cell plating) to monolayers plated in normal medium blocks the surface expression of 184 kD (*A*, ♦) but fails to block the Ca^{++}-induced externalization of the 184-kD protein when added together with the Ca^{++} to monolayers maintained for 24 h in 1–5 μM Ca^{++} (*B*, ♦). This suggests that ~60% of the 184-kD protein synthesized in 1–5 μM Ca^{++} is stored in an intracellular compartment, which is induced to exocytosis in the presence of 1.8 mM Ca^{++}.

Addition of Ca^{++} to Open Monolayers Causes Exocytosis of the 184-kD Protein Stored in the Intracellular Pool

Previous work mentioned about (23, 64) has shown that restoration of normal Ca^{++} levels to open monolayers allows reestablishment of both lateral surface and tight junctions within 2–4 h. Addition of Ca^{++} to open monolayers resulted also in additional surface expression of the 184-kD protein, which reached levels of control (+ Ca^{++}) monolayers within 12 h (solid circles in Fig. 2 *B*). The observation that cycloheximide did not initially (during the first 6 h) block this Ca^{++}-induced surface expression (solid diamonds Fig. 3 *B*) suggests that the source of most of this antigen was the large intracellular pool described before. After 6 h, cycloheximide did cause a progressive decrease in the surface expression of the 184-kD protein, presumably due to antigen turnover (solid diamonds in Fig. 3 *B*). On the other hand, cycloheximide added immediately after typsinization and plating blocked, as expected, the surface expression of the antigen (solid diamonds in Fig. 3 *A*). These results indicate that a significant intracellular pool of the 184-kD protein in open monolayers is available for delivery to the cell surface after Ca^{++}, and normal cell–cell interactions, are restored.

Determination of the intracellular calcium concentration by quin2 fluorescence (5, 62, 63) showed values of 185 nM for cells kept in DME and 170 nM for cells kept in 1–5 μM

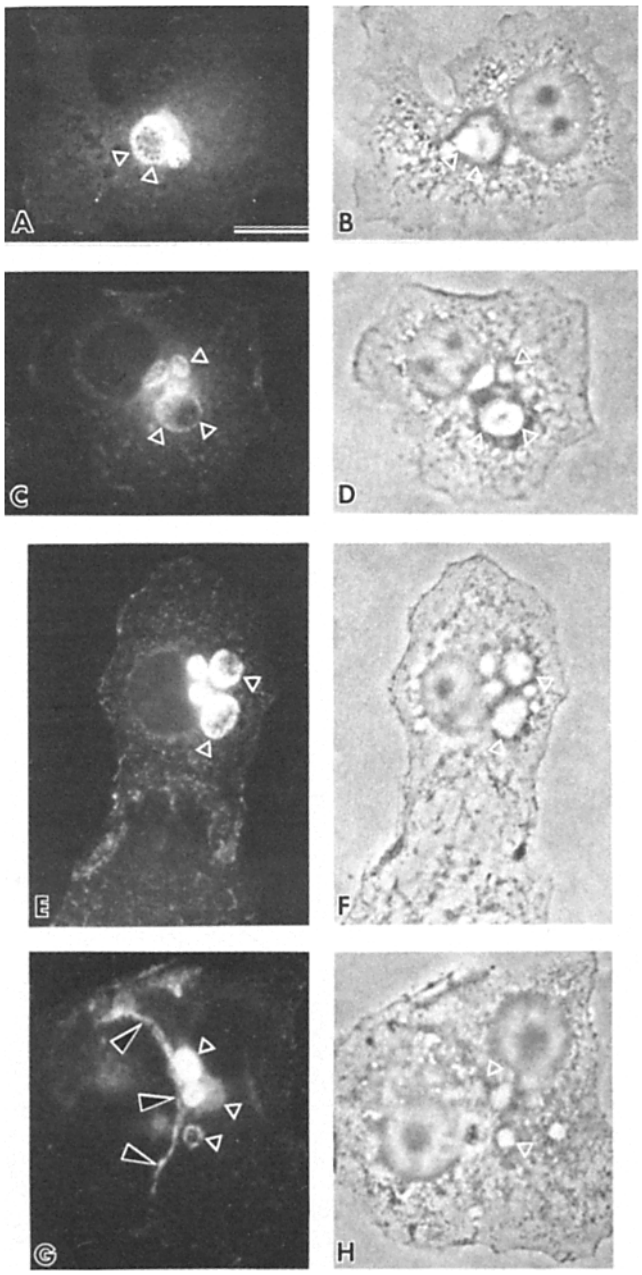

Figure 4. Immunofluorescence localization of the 184-kD intracellular compartment. Subconfluent MDCK monolayers were incubated in DME for 17 h, fixed in 2% paraformaldehyde/0.1% glutaraldehyde. The cells were processed with mAb against 184-kD protein and nonfluorescent second antibodies to quench the surface fluorescence. The cells were then permeabilized with 0.1% saponin and processed for immunofluorescence with the same monoclonal antibody and rhodaminated goat anti-mouse IgG. The vacuoles containing 184-kD (*small arrowheads*) are shown in single cells (*A–D*) and in cell pairs (*E–H*). In this case, the vacuoles often appeared close to cell–cell boundaries (*large arrowheads* in *G*). Bar, 5 μm.

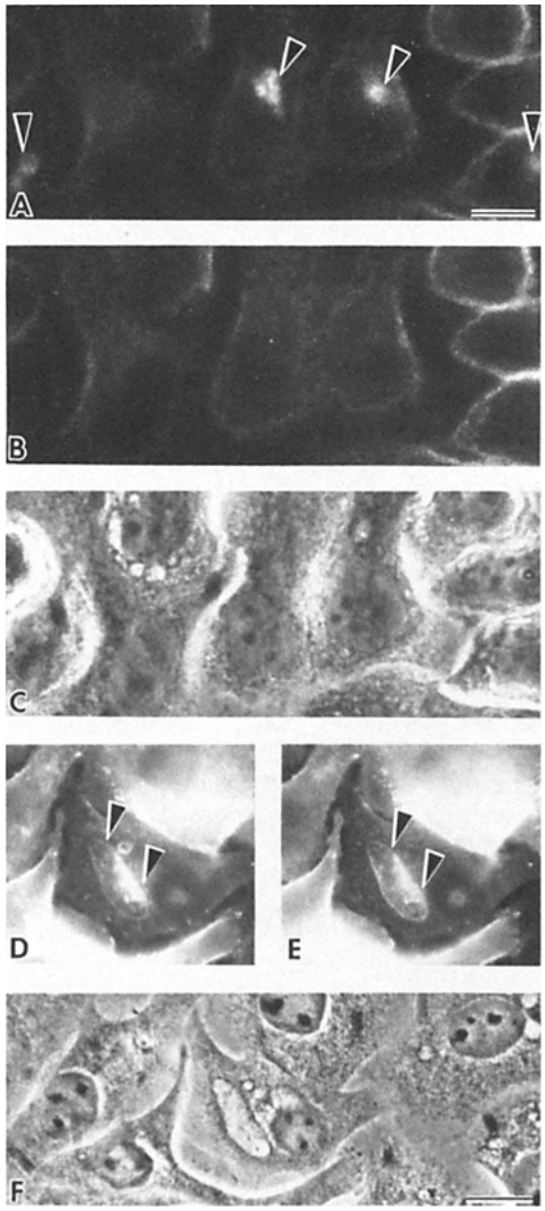

Figure 5. Immunofluorescence localization of the 184-kD protein, influenza virus hemagglutinin, and a basolateral cellular membrane protein. Confluent MDCK cell monolayers were kept in S-MEM for 24 h and fixed in 2% paraformaldehyde/0.1% glutaraldehyde. The cells were incubated with first antibodies and nonfluorescent second antibodies in order to partially quench the surface fluorescence and then permeabilized with 0.1% saponin and processed for indirect immunofluorescence. Monolayers shown in *A* and *B* were incubated sequentially in mAb against 184-kD protein, affinity-purified fluorescein-coupled goat anti-mouse IgG, mAb against a basolateral 63-kD cell membrane protein, and rhodamine-coupled goat anti-mouse IgG. (*A*) The fluorescein immunofluorescence showed intracellular structures (*arrowheads*) of variable sizes (0.5–5 μm) containing 184 kD. (*B*) The rhodamine immunofluorescence of the same cells in the same focal plane showed a clear colocalization of both cellular antigens on the cell surface but no 63-kD protein in the intracellular compartment. (*C*) Phase-contrast image corresponding to *A* and *B*. (*D* and *E*) MDCK cells kept for 24 h in low calcium medium were infected with influenza A virus (WSN, ts61) in the same medium and fixed 6 h later as described above. The cells were processed for immunofluorescence using 184-kD mAb and an affinity-purified polyclonal anti-influenza hemagglutinin rabbit IgG in the first step, and affinity-purified rhodaminated goat anti-mouse IgG and fluoresceinated goat anti-rabbit IgG in the second step. (*D*) The rhodamine fluorescence showed the localization of the 184-kD protein in a large intracellular structure (*arrowheads*). (*E*) The fluorescein fluorescence showed influenza hemagglutinin in the same intracellular structure. The colocalization of both proteins (hemagglutinin and the 184-kD protein) was almost perfect except for a small vesicular structure (between arrowheads) that was positive only for the 184-kD protein. (*F*) Phase-contrast image corresponding to *D* and *E*. Bars, 5 μm.

Ca^{++}. This small (8%) difference rules out the possibility that reduced intracellular Ca^{++} levels are a signal for intracellular storage of the 184-kD protein in cells kept in 1–5 μM Ca^{++}. Rather, it suggests that the absence of cell–cell interactions acts through intracellular messages other than Ca^{++} to produce intracellular storage.

The Intracellular Storage Compartment of the 184-kD Protein Is Composed of Large Vacuolar Structures

Work from other laboratories indicates that confluency promotes the expression of apical epithelial functions (43, 68). If, as suggested by the results described above, epithelial cells lacking intercellular contacts store apical components intracellularly, conditions which reduce or abolish cell–cell interactions should result in the detection of structures containing apical antigens. This was, indeed, observed. In single cells from subconfluent monolayers fixed 17 h after plating, the 184-kD protein was observed localized in large juxtanuclear vacuoles (1–4 per cell; 0.5–5.0 μm in size) which were also clearly visible by phase-contrast microscopy (Fig. 4, *A–D*). Approximately 15% of the cells exhibited vacuolar structures which were visualized both by immunofluorescence and phase-contrast microscopy; as shown below, this may be in fact a large underestimation of the real number of vacuolar structures detectable by immunoelectron microscopy. In cell pairs, vacuoles recognizable by both fluorescence and phase-contrast microscopy were observed at half the frequency observed in single cells; usually only one of the cells exhibited these structures (Fig. 4, *E–H*), while the other cell often had a higher level of surface fluorescence (not shown). In groups of two or more cells, the frequency decreased drastically and generally only cells with the smallest amount of shared membrane displayed vacuolar structures positive for the 184-kD protein (Fig. 4, *E–H*). Vacuoles in cell groups were usually localized near regions of cell–cell contact (Fig. 4, *G* and *H*), suggesting that exocytosis of the vacuoles might take place at this level (see also Fig. 7 *A*, *inset*).

As expected, immunofluorescence examination of confluent monolayers kept in 1–5 μM Ca^{++} demonstrated a large proportion of cells (~50%) displaying large, usually single, phase-positive vacuoles containing the 184-kD protein (Fig. 5, *A* and *D*; see morphometric details below). As shown below, this number clearly underestimates the actual percent of cells expressing the vacuoles at the electron microscopic level. No vacuoles were observed in confluent monolayers developed in normal calcium medium. Addition of 1.8 mM calcium to monolayers previously kept in 1–5 μM Ca^{++} caused a 50% decrease in the number of vacuoles within the first 2 h and an 88% decrease within 24 h.

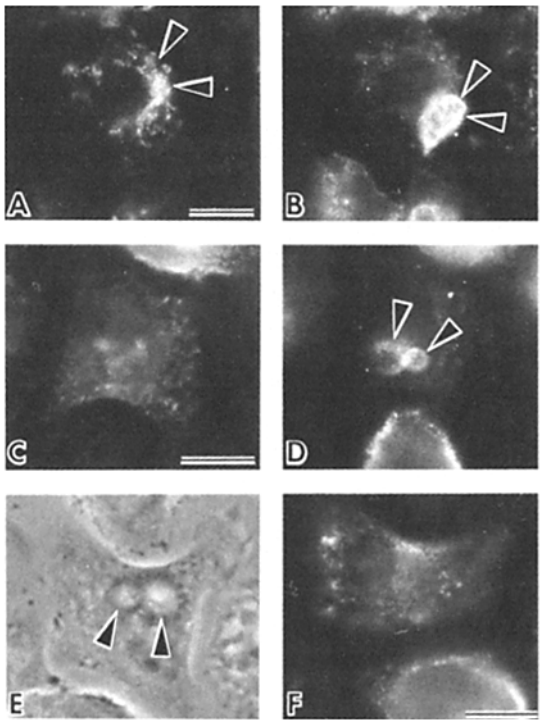

Figure 6. Exclusion of VSV G protein from the intracellular storage compartment. MDCK cells infected with VSV (ts045) virus were shifted to the permissive temperature for 50 min and processed as described in Fig. 5 for immunofluorescence with affinity-purified rabbit anti-G protein and fluorescein-coupled goat anti-rabbit IgG (fluorescein filter) (*A*, *C*, and *F*) and with anti-184-kD protein mAb and rhodamine-coupled anti-mouse IgG (rhodamine filter) (*B* and *D*). To control for surface expression of G protein, MDCK cells were infected and processed in parallel but the surface fluorescence was not quenched and the cells were not detergent permeabilized (*F*). (*A*) The arrowheads point at the Golgi complex positive for G protein 50 min after shifting the cells to the permissive temperature. (*B*) The arrowheads point at an apical membrane vacuole clearly showing different distribution of the cellular 184-kD protein in the same cell. G protein is also excluded from the vacuole in a cell showing positive surface fluorescence (*C*). *D* shows the fluorescence for 184-kD protein in the same cell. (*E*) Phase-contrast image corresponding to *C* and *D*. Bars, 5 μm.

The Vacuolar Compartment That Stores the 184-kD Protein Includes Other Apical MDCK Markers, But Excludes Basolateral Proteins

Double immunofluorescence localization experiments on monolayers kept in 1–5 μM Ca^{++} showed that the large intracellular vacuoles storing the 184-kD protein excluded a 63-kD basolateral MDCK marker (Fig. 5 *B*) (65). Similar experiments indicated that they also excluded the basolaterally targeted VSV G protein (Fig. 6, *A–D*), at a time (50 min after temperature shift) when all the cells in parallel monolayers showed clear surface fluorescence (Fig. 6 *F*) for G protein. On the other hand, the vacuoles included influenza HA, an apically directed viral glycoprotein (Fig. 5, *D* and *E*). Although these results were similar in all cells, only cells with lower levels of surface expression of HA, G protein, or 184-kD protein allowed adequate photography of the vacuoles. The surface fluorescence was partially quenched incubating the cells with nonfluorescent antibodies before detergent permeabilization (except in Fig. 6 *F*).

As shown in a previous work (64), the 63-kD antigen was observed on the apical surface of the cells in low Ca^{++} medium (i.e., not polarized, see also Fig. 5 *B*), indicating that the sorting of apical and basolateral proteins is imperfect at the cell surface level operates with a higher degree of fidelity for the intracellular storage compartment. Because of its capacity to store apical membrane proteins and exclude basolateral ones, we call this intracellular structure the vacuolar apical compartment (VAC).

VAC Has Morphological Features of the Apical Membrane

After staining monolayers kept in 1–5 μM Ca^{++} with an EM immunoperoxidase procedure, VAC was observed to be composed of intracellular vacuoles containing many microvilli (Fig. 7, *A*, *B*, *F*, and *H*). Using standard morphometric techniques (see Materials and Methods) that account for the size of the vacuoles and the frequency of appearance in the cell sections, we estimated that VAC has a surface area of 2,500 μm^2/cell, or ~61% of the total plasma membrane area, and is seen in at least 92% of the cells (Table I). Double localization experiments showed that VAC excluded cationized ferritin added to the medium (Fig. 7, *C*, *E–H*) indicating that these large vacuoles constitute a real intracellular compartment rather than invaginations of the plasma membrane. In similar experiments the cells were incubated at 37°C with cationized ferritin for various times (ranging 2 to 24 h) after dissociation and plating. VAC appeared at 12 to 20 h and always excluded cationized ferritin (not shown) suggesting that it is not formed as a result of massive internalization of apical membrane.

Effect of the Substratum on Expression of the 184-kD Protein

To distinguish the effects of cell–cell contacts from cell–substratum interactions on the synthesis and surface expression of the 184-kD protein, MDCK cells were incubated within agarose gels (to which they do not attach) or native type I

Table I. Morphometric Measurements of the 184-kD Protein Intracellular Compartment

Membrane surfaces (μm^2/cell)		
Plasma membrane	4,051 ± 1,225	100%
Intracellular vacuole	2,531 ± 3,668	61%
Intracellular vacuole parameters		
Large diameter	3.6 ± 1.3 μm	
Small diameter	0.9 ± 0.4 μm	
Mean caliper D	3.3 μm	
N_v	2.7×10^{-4} μm^{-3}	
Vacuoles/cell	0.92	

Independent (nonserial) sections of 25 MDCK cells stained with S2/2GI mAb (anti-184-kD protein)/peroxidase were measured as described in Materials and Methods. The criteria to define intracellular vacuoles were (*a*) the presence of microvilli, and (*b*) positive peroxidase reaction for the 184-kD protein. Only nine sections showed an intracellular vacuole. N_v is the number/volume density. Since under these conditions the vacuoles were mostly single, N_v × mean cell volume = vacuoles/cell.

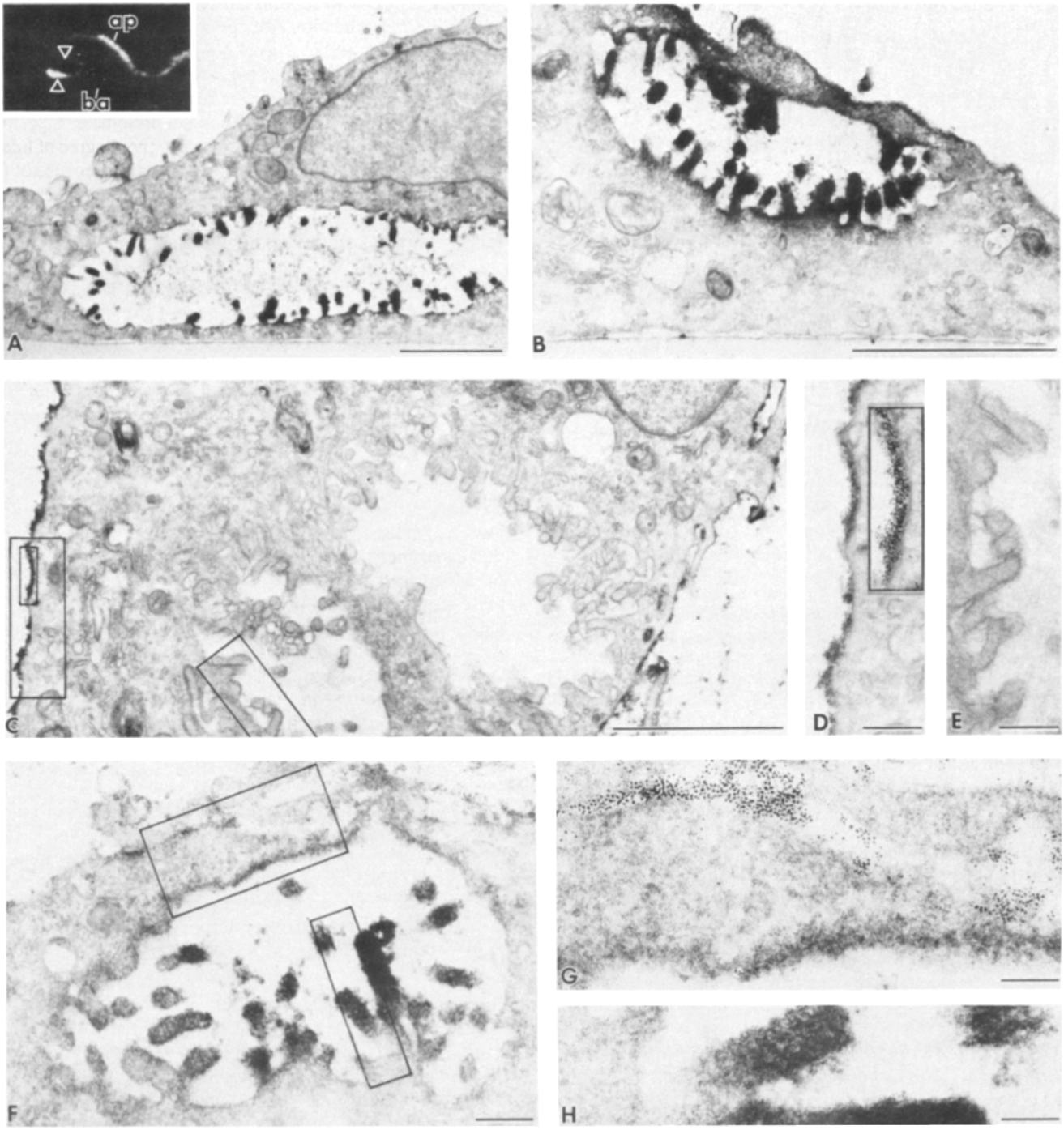

Figure 7. Immunoelectron microscopy localization of the 184-kD protein in MDCK cells grown in low calcium medium. MDCK cell monolayers were kept for 24 h in low calcium medium. Some monolayers were incubated in S-MEM supplemented with 1 mg/ml cationized ferritin for 1 h at 14°C (*C–G*). The cells were fixed in 3% paraformaldehyde/0.1% glutaraldehyde, or in 2% glutaraldehyde in 0.2 M cacodylate buffer (*C–E*). All the samples were processed for immunoperoxidase with the anti-184-kD mAb, affinity-purified anti-mouse rabbit IgG, and affinity-purified anti-rabbit goat IgG (Fab fragment) coupled to horseradish peroxidase, except for those in *C–E*. The peroxidase reaction was developed in the presence of diaminobenzidine and the cells were processed for electron microscopy. (*Inset* in *A*) The semi-thin frozen section of an MDCK cell processed for immunofluorescence with anti-184-kD mAb; the arrowheads are pointing at a vacuole. The 184-kD protein localized in large intracellular vacuoles giving a clearly positive peroxidase reaction (*A*, *B*, *F–H*). The vacuoles had microvilli, which are mostly absent from the cell surface. Some cells showed positive surface reaction (*B*) while others did not (*A*). Cationized ferritin added before fixation (*C*, *D*, *F*, and *G*) was never found inside the large vacuolar structures (*C*, *E*, *G*, and *H*). Bars: (*A–C*) 1 μm; (*D–F*) 0.25 μm; (*G* and *H*) 0.1 μm.

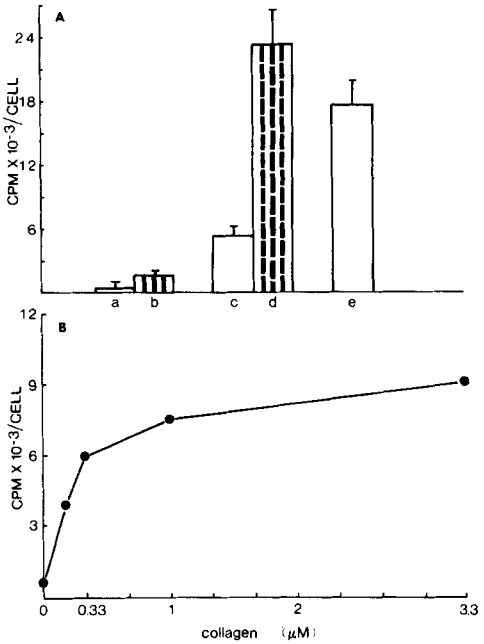

Figure 8. Effect of the substratum on the expression of the 184-kD protein in MDCK cells. (*A*) MDCK cells were dissociated with trypsin EDTA and immediately mixed with 3% ultralow gelling point agarose in MEM at 37°C (*a* and *b*). Some cells were mixed with 2 mg/ml native (ungelled) rat tail collagen (*c* and *d*). The same number of cells was plated in parallel on a native collagen (2 mg/ml) gel to allow them to form a monolayer (*e*). The agarose gels were incubated for 10 min at 4°C to gel the agarose before the cells could sediment in the bottom of the petri dish. The cells were then incubated for 24 h in the 37°C tissue culture incubator, fixed in 3% paraformaldehyde, made permeable (*dashed line bars*) or not (*open bars*) with detergent and processed for indirect RIA with anti-184-kD mAb and affinity-purified [^{125}I]goat anti-mouse IgG. Each antibody incubation or wash was performed in 1.5 h to allow proper diffusion of antibodies through the 1-2-mm-thick agarose gel. The data expressed in cpm/cell are the average from three independent experiments performed on triplicate or quintuplicate monolayers. (*B*) MDCK cells were dissociated and mixed with agarose gels as described above, except for the inclusion of known concentrations of lathyritic (soluble) rat skin collagen (type I). The cells were incubated, fixed, and processed for RIA as described above. In some gels, the cells were made permeable with detergent (*b* and *d*). The specific binding, expressed in cpm/cell, is shown as a function of the collagen concentration. Note that the expression of 184-kD protein is a saturable function of collagen concentration.

collagen gels (a good substratum for MDCK cells). Under these conditions, cells remained apart but viable for longer than 15 h. Isolated MDCK cells included in agarose expressed very low levels of the 184-kD protein, as detected by RIA (Fig. 8, *A*, bars *a* and *b*) or immunofluorescence (Fig. 9, *A* and *B*). Lower levels of surface expression of the 184-kD protein were observed in single cells than in cell pairs (Fig. 9, *A* and *B*), presumably due to exocytosis of intracellular antigen triggered by cell-cell interactions. On the other hand, MDCK cells included in a collagen gel exhibited 15-fold and 14-fold higher levels of surface and total cell antigen, respectively. Under both agar and collagen inclusion culture conditions, the majority of the 184-kD protein was intracellular (Fig. 8, *A*, bars *b* and *d*). As predicted from RIA experiments, the surface fluorescence was much higher in isolated

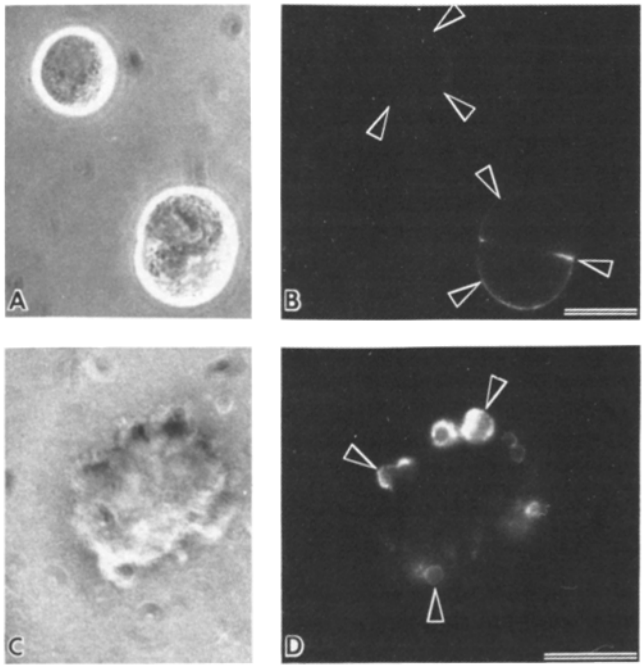

Figure 9. Immunofluorescence localization of the 184-kD membrane protein in MDCK cells embedded in agarose or collagen gels. MDCK cells were dissociated, incubated within agarose or collagen gels as described in Fig. 7 *A*, and then fixed and processed for indirect immunofluorescence. Arrowheads point at the cell surface of cells within an agarose gel (*A* and *B*) and at cell surface blebs positive for 184-kD apical protein in cells within a collagen gel (*C* and *D*). Bars, 10 μm.

MDCK cells included within collagen gels (Fig. 9, *C* and *D*). Interestingly, in this case, the 184-kD antigen was concentrated in membrane blebs. Increasing collagen concentration within the gel resulted in increasing levels of the 184-kD protein with saturation being reached at ~300 nM collagen (Fig. 8 *B*). Thus, while the synthesis of 184-kD protein depends on the presence of an adequate substratum, such as collagen, its distribution between cell surface and intracellular storage pools is regulated by specific cell-cell interactions.

Discussion

The results reported here indicate that MDCK cells replated after trypsin dissociation under three experimental conditions that abolish or reduce cell-cell interactions (subconfluent culture, 1-5 μM Ca^{++} and inclusion within agarose or collagen gels) display an intracellular storage compartment for apical membrane proteins. This compartment (VAC) was found under two different conditions of fixation (Fig. 7) and shares morphological and biochemical properties with the apical surface of polarized monolayers of epithelial cells. First, it contains typical microvilli. Second, it expresses cellular and viral apical glycoproteins (184-kD protein and influenza hemagglutinin). Third, it excludes typical basolateral proteins (63-kD protein and VSV G protein). To our knowledge, this is the first description of such an epithelial cell organelle.

A mechanism to store apical proteins intracellularly when the epithelium is not ready to perform a differentiated function (for example during cell growth) might be convenient for

the cell to "get ready" to quickly carry out its tissue-specific function once the external conditions become "appropriate." Similar mechanisms have been observed in stomach (31) and urinary bladder (46) epithelia that externalize intracellularly stored apical membrane components under hormonal stimulation in order to carry out specific functions.

Although epithelial cells in normal adult tissues form continuous monolayers, clear examples of loss of intercellular contact between epithelial cells which may lead in vivo to the appearance of VAC structures are present during development and in pathological processes. The kidney is formed from metanephric mesenchymal cells that undergo epithelial differentiation (14, 15, 57). Typical pathologic processes which result in disconnected or mobile epithelial cells are invasive carcinomas and after acute kidney tubular necrosis (36, 45). Further studies are needed to determine whether intracellular storage of apical proteins by VAC is characteristic in these cases.

Role of Cell–Cell Contacts in the Exocytosis of VAC

Our results indicate that the establishment of cell–cell contacts is the critical event that signals the exocytosis of VAC. At present, we do not know which, of the many intercellular adhesive forces, is directly responsible for this event. From a purely morphologic point of view, MDCK cells display tight junctions, intermediate junctions, desmosomes (8, 9), and gap junctions (10). Uvomorulin-like molecules are present in MDCK cells (2, 25) and it is reasonable to expect that future research will identify cell adhesion molecules described in other tissues (6, 13, 44, 60). We found no evidence for a role of intracellular calcium in the exocytosis of VAC. On the other hand, the requirement for extracellular Ca^{++} appears to be related to its role in many junctional and nonjunctional intercellular adhesive mechanisms. Since VAC appeared in subconfluent cells in normal Ca^{++} medium, it is reasonable to conclude that the effect of Ca^{++} is exerted only at the level of cell–cell contacts. More experimental work is required to identify which specific cell adhesion molecule is involved in the exocytosis of VAC.

Sorting of Apical and Basolateral Proteins by VAC and Implications for the Biogenesis of Epithelial Cell Polarity

Two apically located membrane proteins colocalized within the intracellular storage compartment (Fig. 6) while two basolateral membrane proteins did not. Thus, VAC sorts apical from basolateral proteins. This was found to be true even under conditions that disrupt sorting at the cell surface level. In 1–5 μM Ca^{++} basolateral markers invade the apical surface (29, 64, 69) but not the VAC compartment. These findings have clear implications regarding the biogenesis of epithelial polarity. They suggest that the basic mechanisms responsible for vectorial delivery of apical proteins, a property described in confluent, fully polarized monolayers (35, 40), also exist in subconfluent cells (which have no functional tight junctions). They also highlight the postulated "fence" role of tight junctions (25), which would be required to keep basolateral antigens out of the apical surface when this is continuous with the basolateral membrane. VACs, which are in essence isolated "apical membrane," obviously do not need tight junctions to exclude basolateral proteins. Thus, tight junctions are not essential for vectorial exocytosis, but may play a role in keeping molecules segregated once they are inserted.

There are two possible origins of VAC structures: internalization of apical plasma membrane after cell dissociation or de novo membrane synthesis. In epidermal cells, cell dissociation with proteases results in the internalization of desmosomes within vacuoles (20, 41). If VAC is produced de novo it must be from a compartment distal to the Golgi apparatus, perhaps the 20°C subcompartment (24), where sorting of basolateral and apical membrane proteins is thought to take place (35, 40, 48, 50, 56). In fact, unpublished experiments in which MDCK cells were incubated for long periods with cationized ferritin after cell dissociation, suggest that VAC is formed de novo.

Cell–Substratum Interactions

Our results indicate that cell–substratum interactions promote the synthesis of the apical 184-kD protein. This is in agreement with previous findings in other systems which have demonstrated an inductive effect of the substratum on the synthesis of specific cell products (4, 19, 27, 32, 33, 37–39, 59). This mechanism seems to be independent from the presence of cell–cell contacts since high levels of 184-kD protein synthesis, comparable to those observed in confluent monolayers, were detected in cells included in collagen gels.

The culture of epithelial cells within collagen gels has been shown before to cause changes in the spatial orientation of the cells (11, 26). In this work, we found a peculiar distribution of the 184-kD protein on the surface of cells surrounded by collagen: the protein appeared concentrated in surface blebs. The blebs may represent patches of apical surface which become segregated from the regions of cell–collagen interaction (presumably, the remaining antigen-negative areas), similarly to the polarization of the 184-kD protein to free regions of isolated MDCK cells plated on collagen substrata (53, 64).

In summary, we have described an organelle–VAC–involved in the storage of apical proteins in MDCK (epithelial) cells. VAC becomes evident in cells that have not yet developed (or have been experimentally prevented from establishing) cell–cell contacts. Future work should explore how extensively VAC-like structures participate in the biogenesis of the apical surface during epithelium differentiation.

We are grateful to Drs. Doris Wall, Donald A. Fischman, and Joel Pardee for critically reviewing the manuscript; to Dr. Enrique Rabellino for preliminary cell sorting data; to Dr. Doris Herzlinger (Columbia University, New York) for help during characterization of monoclonal antibodies; and to Mr. Wayne Fryes for excellent technical assistance with the electron microscopy.

This work was supported by grants from National Institutes of Health (GM34107) and National Science Foundation (PCM-8217405). E. Rodriguez-Boulan was recipient of a career award from the Irma T. Hischl Trust and an Established Investigator award from the American Heart Association.

Received for publication 31 October 1986, and in revised form 30 December 1986.

Note Added in Proof. Dr. M. Neutra brought to our attention that during development of rat intestinal epithelium, secondary intercellular lumina, resembling the structures described in Fig. 4 *G* in this paper, are observed (Colony, P. C., and M. R. Neutra, 1983, *Dev. Biol.*, 97:349–363).

References

1. Amsler, K., and J. S. Cook. 1982. Development of Na^+-dependent hexose transport in a cultured cell line of porcine kidney cells. *Am. J. Physiol.* 242(Cell Physiol. 11):C94–C101.
2. Behrens, J., W. Birchmeier, S. L. Goodman, and B. A. Imhof. 1985. Dissociation of Madin–Darby canine kidney epithelial cells by the monoclonal antibody anti-Arc-1: mechanistic aspects and identification of the antigen as a component related to uvomorulin. *J. Cell Biol.* 101:1307–1315.
3. Ben-Ze'ev, A. 1984. Differential control of cytokeratins and vimentin synthesis by cell–cell contact and cell spreading in cultured epithelial cells. *J. Cell Biol.* 99:1424–1433.
4. Ben-Ze'ev, A., S. R. Farmer, and S. Penman. 1980. Protein synthesis requires cell-surface contact while nuclear events respond to cell shape in anchorage-dependent fibroblasts. *Cell.* 21:365–372.
5. Bitar, K. N., P. Bradford, J. W. Putney, Jr., and G. M. Makhlouf. 1986. Cytosolic calcium during contraction of isolated mammalian gastric muscle cells. *Science (Wash. DC).* 232:1143–1145.
6. Braslau, D. L., D. L. Ringo, and V. Rocha. 1984. Synthesis of novel calcium-dependent proteins associated with mammary epithelial cell migration and differentiation. *Exp. Cell Res.* 155:213–221.
7. Brown, W. J., and M. G. Farquhar. 1984. The mannose-6-phosphate receptor for lysosomal enzymes in concentrated in *Cis* Golgi cisternae. *Cell.* 36:295–307.
8. Cereijido, M., J. Ehrenfeld, I. Meza, and A. Martinez-Palomo. 1980. Structural and functional membrane polarity in cultured monolayers and MDCK cells. *J. Membr. Biol.* 52:147–159.
9. Cereijido, M., E. S. Robbins, W. J. Dolan, C. A. Rotuno, and D. D. Sabatini. 1978. Polarized monolayers formed by epithelial cells on a permeable and transluscent support. *J. Cell Biol.* 77:853–880.
10. Cereijido, M. E. Robbins, D. D. Sabatini, and E. Stefani. 1984. Cell-to-cell communication in monolayers of epithelioid cells (MDCK) as a function of the age of the monolayer. *J. Membr. Biol.* 81:41–48.
11. Chambard, M., J. Gabrion, and J. Mauchamp. 1981. Influence of collagen gel on the orientation of epithelial cell polarity: follicle formation from isolated thyroid cells and from preformed monolayers. *J. Cell Biol.* 91:157–166.
12. Chung, S., S. M. Landfear, D. D. Blumberg, N. S. Cohen, and H. F. Lodish. 1981. Synthesis and stability of developmentally regulated *Dictyostelium* mRNAs are affected by cell-cell contact and cAMP. *Cell.* 24: 785–797.
13. Crossin, K. L., C. M. Chuong, and G. M. Edelman. 1985. Expression sequences of cell adhesion molecules. *Proc. Natl. Acad. Sci. USA.* 82: 6942–6946.
14. Ekblom, P., K. Alitalo, A. Vaheri, R. Timpl, and L. Saxen. 1980. Induction of a basement membrane glycoprotein in embryonic kidney: possible role of laminin in morphogenesis. *Proc. Natl. Acad. Sci. USA.* 77: 485–489.
15. Ekblom, P., E. Lehtonen, L. Saxen, and R. Timpl. 1981. Shift in collagen type as an early response to induction of the metanephric mesenchyme. *J. Cell Biol.* 89:276–283.
16. Elsdale, T., and J. Bard. 1972. Collagen substrata for studies on cell behavior. *J. Cell Biol.* 54:626–637.
17. Emerman, J. T., S. J. Burwen, and D. R. Pitelka. 1979. Substrate properties influencing ultrastructural differentiation of mammary epithelial cells in culture. *Tissue & Cell.* 11:109–119.
18. Enat, R., D. M. Jefferson, N. Ruiz-Opazo, Z. Gatmaitan, L. A. Leinwand, and L. M. Reid. 1984. Hepatocyte proliferation in vitro: its dependence on the use of serum-free hormonally defined medium and substrata of extracellular matrix. *Proc. Natl. Acad. Sci. USA.* 81:1411–1415.
19. Farmer, S. R., A. Ben-Ze'ev, B.-J. Benecke, and S. Penman. 1978. Altered translatability of messenger RNA from suspended anchorage-dependent fibroblasts: reversal upon cell attachment to a surface. *Cell.* 15:627–637.
20. Fukuyama, K., M. M. Black, and W. L. Epstein. 1974. Ultrastructural studies of newborn rat epidermis after trypsinization. *J. Ultrastruct. Res.* 46:219–229.
21. Gatmaitan, Z., D. M. Jefferson, N. Ruiz-Opazo, L. Biempica, I. M. Arias, G. Dudas, L. A. Leinwand, and L. M. Reid. 1983. Regulation of growth and differentiation of a rat hepatoma cell line by the synergistic interactions of hormones and collagenous substrata. *J. Cell Biol.* 97:1179–1190.
22. Giloh, H., and J. W. Sedat. 1982. Fluorescence microscopy: reduced photobleaching of rhodamine and fluorescein protein conjugates by n-propyl gallate. *Science (Wash. DC).* 217:1252–1255.
23. Gonzalez-Mariscal, L., B. Chavez de Ramirez, and M. Cereijido. 1985. Tight junction formation in cultured epithelial cells (MDCK). *J. Membr. Biol.* 86:113–125.
24. Griffiths, G., S. Pfeiffer, K. Simons, and K. Matlin. 1985. Exit of newly synthesized membrane proteins from the trans cisterna of the Golgi complex to the plasma membrane. *J. Cell Biol.* 101:949–964.
25. Gumbiner, B., and K. Simons. 1986. A functional assay for proteins involved in establishing an epithelial occluding barrier: identification of a uvomorulin-like polypeptide. *J. Cell Biol.* 102:457–468.
26. Hall, H. G., D. A. Farson, and M. J. Bissell. 1982. Lumen formation by epithelial cell lines in response to collagen overlay: a morphogenetic model in culture. *Proc. Natl. Acad. Sci. USA.* 79:4672–4676.
27. Hay, E. D., and S. Meier. 1976. Stimulation of corneal differentiation by interaction between cell surface and extracellular matrix. II. Further studies on the nature and site of transfilter "induction". *Dev. Biol.* 52: 141–157.
28. Heimark, R. L., and S. M. Schwartz. 1985. The role of membrane–membrane interactions in the regulation of endothelial cell growth. *J. Cell Biol.* 100:1934–1940.
29. Herzlinger, D. A., and G. Ojakian. 1984. Studies on the development and maintenance of epithelial cell surface polarity with monoclonal antibodies. *J. Cell Biol.* 98:1777–1787.
30. Hilliard, J. E. 1967. The calculation of the mean caliper diameter of a body for use in the analysis of the number of particles per unit volume. *In* Stereology. H. Elias, editor. Springer-Verlag, New York. 211–215.
31. Hirst, B. H., and J. G. Forte. 1985. Redistribution and characterization of $(H^+$-$K^+)$-ATPase membranes from resting and stimulated gastric parietal cells. *Biochem. J.* 231:641–649.
32. Lee, E. Y-H. P., W-H. Lee, C. S. Kaetzel, G. Parry, and M. Bissell. 1985. Interaction of mouse mammary epithelial cells with collagen substrata: regulation of casein gene expression and secretion. *Proc. Natl. Acad. Sci. USA.* 82:1419–1423.
33. Lee, E.Y-H., G. Parry, and M. J. Bissell. 1984. Modulation of secreted proteins of mouse mammary epithelial cells by the collagenous substrata. *J. Cell Biol.* 98:146–155.
34. Levine, J. F., and F. E. Stockdale. 1985. Cell–cell interactions promote mammary epithelial cell differentiation. *J. Cell Biol.* 100:1415–1422.
35. Matlin, K., and K. Simons. 1984. Sorting of an apical plasma membrane glycoprotein occurs before it reaches the surface in cultured epithelial cells. *J. Cell Biol.* 99:2131–2139.
36. McDowell, E. M., R. B. Nagle, R. C. Zallme, J. S. McNeil, W. Flamabaw, and B. F. Trump. 1976. Studies on the pathophysiology of acute renal failure. I. Correlation of ultrastructure and function in the proximal tubule of the rat following administration of mercuric chloride. *Virchows Arch. B Cell Pathol.* 22:173–196.
37. Meier, S., and E. D. Hay. 1974. Control of corneal differentiation by extracellular materials. Collagen as a promoter and stabilizer of epithelial stroma production. *Dev. Biol.* 38:249–270.
38. Meier, S., and E. D. Hay. 1974. Stimulation of extracellular matrix synthesis in the developing cornea by glycosaminoglycans. *Proc. Natl. Acad. Sci. USA.* 71:2310–2313.
39. Meier, S., and E. D. Hay. 1975. Stimulation of corneal differentiation by interaction between cell surface and extracellular matrix. I. Morphometric analysis of transfilter "induction." *J. Cell Biol.* 66:275–291.
40. Misek, D. E., E. Bard, and E. Rodriguez-Boulan. 1984. Biogenesis of epithelial cell polarity: intracellular sorting and vectorial exocytosis of an apical plasma membrane glycoprotein. *Cell.* 39:537–546.
41. Morejohn, L. C., and J. N. Pratley. 1979. Differential effects of trypsin on the epidermis of Rana catesbiana. Observations on differentiating junctions and cytoskeletons. *Cell Tissue Res.* 198:349–362.
42. Mori, Y., H. Akedo, Y. Tanigaki, K. Tanaka, and M. Okada. 1979. Ciliogenesis in tissue-cultured cells by the increased density of cell population. *Exp. Cell Res.* 120:435–439.
43. Mullin, J. M., J. Weibel, L. Diamond, and A. Kleinzeller. 1980. Sugar transport in the LLC-PKl renal epithelial cell line: similarity to mammalian kidney and the influence of cell density. *J. Cell. Physiol.* 104: 375–389.
44. Odin, P., and B. Obrink. 1986. Dynamic expression of the cell adhesion molecule cell-CAM 105 in fetal and regenerating rat liver. *Exp. Cell Res.* 164:103–114.
45. Olsen, T. S., H. S. Olsen, and H. E. Hansen. 1985. Tubular ultrastructure in acute renal failure in man: epithelial necrosis and regeneration. *Virchows Arch. A Pathol. Anat. Histopathol.* 406:75–89.
46. Parisi, M., and J. Bourguet. 1984. Effects of cellular acidification on ADH-induced intramembrane particle aggregates. *Am. J. Physiol.* 246:c157–c159.
47. Parry, G., E. Y-H. Lee, D. Farson, M. Koval, and M. Bissell. 1985. Collagenous substrata regulate the nature and distribution of glycosaminoglycans produced by differentiated cultures of mouse mammary epithelial cells. *Exp. Cell Res.* 156:487–499.
48. Pfeiffer, S., S. D. Fuller, and K. Simons. 1985. Intracellular sorting and basolateral appearance of the G protein of vesicular stomatitis virus in Madin–Darby canine kidney cells. *J. Cell Biol.* 101:470–476.
49. Rabito, C. A., J. I. Kreisberg, and D. Wight. 1984. Alkaline phosphatase and gamma-glutamyl transpeptidase as polarization markers during the organization of LLC-PKl cells into an epithelial membrane. *J. Biol. Chem.* 259:574–582.
50. Rindler, M. J., I. E. Ivanov, H. Plesken, E. Rodriguez-Boulan, and D. D. Sabatini. 1984. Viral glycoproteins destined for apical or basolateral plasma membrane domains traverse the same Golgi apparatus during their intracellular transport in doubly infected Madin–Darby canine kidney cells. *J. Cell Biol.* 98:1304–1319.
51. Rodriguez-Boulan, E. 1983. Membrane biogenesis, enveloped RNA viruses, and epithelial polarity. *Mod. Cell Biol.* 1:119–170.
52. Rodriguez-Boulan, E. 1983. Polarized assembly of enveloped viruses from cultured epithelial cells. *Methods Enzymol.* 98:486–501.

53. Rodriguez-Boulan, E., K. T. Paskiet, and D. D. Sabatini. 1983. Assembly of enveloped viruses in Madin–Darby canine kidney cells: polarized budding from single attached cells and from clusters of cells in suspension. *J. Cell Biol.* 96:866–874.
54. Rodriguez-Boulan, E., K. T. Paskiet, P. J. I. Salas, and E. Bard. 1984. Intracellular transport of influenza virus hemagglutinin to the apical surface of Madin–Darby canine kidney cells. *J. Cell Biol.* 98:308–319.
55. Salas, P. J. I., D. E. Misek, D. E. Vega-Salas, D. Gundersen, M. Cereijido, and E. Rodriguez-Boulan. 1986. Microtubules and actin microfilaments are not critically involved in the biogenesis of epithelial cell surface polarity. *J. Cell Biol.* 102:1853–1867.
56. Salas, P. J. I., D. E. Vega-Salas, D. Misek, E. Bard, and E. Rodriguez-Boulan. 1984. Intracellular sorting of plasma membrane glycoproteins in epithelial cells. *Ann. N.Y. Acad. Sci.* 435:337–340.
57. Saxen, L., O. Koskimies, A. Lahti, H. Miettinen, J. Rapola, and J. Wartiovaara. 1968. Differentiation of kidney mesenchyme in an experimental model system. *Adv. Morphog.* 7:251–293.
58. Simons, K., and S. D. Fuller. 1985. Cell surface polarity in epithelia. *Annu. Rev. Cell Biol.* 1:243–288.
59. Sugrue, S. P., and E. D. Hay. 1986. The identification of extracellular matrix (ECM) binding sites on the basal surface of embryonic corneal epithelium and the effect of ECM binding on epithelial collagen production. *J. Cell Biol.* 102:1907–1916.
60. Thiery, J. P., A. Delouvee, W. J. Gallin, B. A. Cunningham, and G. M. Edelman. 1984. Ontogenic expression of cell adhesion molecules: L-CAM is found in epithelia derived from the three primary germ layers. *Dev. Biol.* 102:61–78.
61. Towbin, H., T. Staehelin, and J. Gordon. 1979. Electrophoretic transfer of proteins from polyacrylamide gels to nitrocellulose sheets: procedure and some applications. *Proc. Natl. Acad. Sci. USA.* 76:4350–4354.
62. Tsien, R. Y. 1981. A non-disruptive technique for loading calcium buffers and indicators into cells. *Nature (Lond.).* 290:527–528.
63. Tsien, R. Y., T. Pozzan, and T. J. Rink. 1982. Calcium homeostasis in intact lymphocytes: cytoplasmic free calcium monitored with a new, intracellularly trapped fluorescent indicator. *J. Cell Biol.* 94:325–334.
64. Vega-Salas, D. E., P. J. I. Salas, D. Gundersen, and E. Rodriguez-Boulan. 1987. Formation of the apical pole of epithelial Madin–Darby canine kidney cells: polarity of an apical protein is independent of tight junctions while segregation of a basolateral marker requires cell–cell interactions. *J. Cell Biol.* 104:905–916.
65. Vega-Salas, D. E., P. J. I. Salas, and E. Rodriguez-Boulan. 1985. Monoclonal antibodies against apical surface antigens of MDCK (epithelial) cells. *J. Cell Biol.* 101(5, Pt. 2):61*a*. (Abstr.)
66. Weibel, E. R. 1969. Stereological principles for morphometry in electron microscopic cytology. *Int. Rev. Cytol.* 26:235–302.
67. Wicha, M. S., G. Lowrie, E. Kohn, P. Bagavandoss, and T. Mahn. 1982. Extracellular matrix promotes mammary epithelial growth and differentiation in vitro. *Proc. Natl. Acad. Sci. USA.* 79:3213–3217.
68. Yoneyama, Y., and J. E. Lever. 1984. Induction of microvillar hydrolase activities by cell density and exogenous differentiation inducers in an established kidney epithelial cell line (LLC-PK1). *J. Cell. Physiol.* 121: 64–73.
69. Ziomek, C. A., S. Schulman, and M. Edidin. 1980. Redistribution of membrane proteins in isolated mouse intestinal epithelial cells. *J. Cell Biol.* 86:849–857.